buildings

MDPI

Article

Properties and Tensile Softening Laws of Hybrid Basalt Fiber Reinforced Recycled Aggregate Concrete

Shahrukh Shoaib, Hilal El-Hassan and Tamer El-Maaddawy *

Department of Civil and Environmental Engineering, College of Engineering, Al Ain Campus, United Arab Emirates University, Al Ain P.O. Box 15551, United Arab Emirates
* Correspondence: tamer.maaddawy@uaeu.ac.ae

Abstract: The performance of hybrid basalt fiber (BF)-reinforced concrete made with recycled concrete aggregates (RCAs) and dune sand as an eco-friendly construction material is examined. Test variables comprised the base concrete grade (normal- and high-strength concrete (NSC and HSC)), the hybrid BF volume fraction (v_f = 1.0 and 1.5%), and the RCA replacement percentage (30, 60, and 100%). The workability of the concrete mixtures was evaluated via the slump test. The mechanical properties were assessed using compression, splitting tensile, and four-point flexural tests. The durability characteristics were examined using bulk resistivity and ultrasonic pulse velocity (UPV) tests. The addition of hybrid BFs was detrimental to the slump and compressive strength of the concrete mixtures. In contrast, improvements of up to 32 and 40% were recorded in the splitting and flexural strengths of NSC mixtures made with 30–100% RCA. The HSC mixtures exhibited respective improvements of up to 26 and 34% at RCA replacement percentages of 30–60%. The bulk resistivity and UPV values of NSC and HSC mixtures remained almost unaltered with the addition of hybrid BFs. New idealized tensile softening laws were developed for RCA–based concrete reinforced with hybrid BFs. The tensile softening laws were implemented into numerical models that simulated the flexural behavior of the tested concrete prisms with good accuracy.

Keywords: hybrid basalt fibers; recycled concrete aggregates; tensile softening

check for updates

Citation: Shoaib, S.; El-Hassan, H.; El-Maaddawy, T. Properties and Tensile Softening Laws of Hybrid Basalt Fiber Reinforced Recycled Aggregate Concrete. *Buildings* **2023**, *13*, 975. https://doi.org/10.3390/buildings13040975

Academic Editor: Oldrich Sucharda

Received: 2 March 2023
Revised: 4 April 2023
Accepted: 5 April 2023
Published: 6 April 2023

Copyright: © 2023 by the authors. Licensee MDPI, Basel, Switzerland. This article is an open access article distributed under the terms and conditions of the Creative Commons Attribution (CC BY) license (https://creativecommons.org/licenses/by/4.0/).

1. Introduction

The demolition of concrete structures produces an extensive amount of construction and demolition waste (CDW), which is considered a potential threat to the environment if disposed of in landfills [1–4]. It is, therefore, essential to manage the CDW in an appropriate manner. The conversion of CDW into recycled concrete aggregates (RCAs) for subsequent use in concrete structures is considered a sustainable and economical solution for managing CDW [5,6]. The incorporation of locally abundant dune sand as fine aggregates into concrete mixtures containing RCAs would further maximize the environmental benefits and foster sustainability in the construction industry. Dune sand is available in many countries in various continents (e.g., north Africa; the gulf region in Asia, France in Europe, western Australia, the United States in North America). Concrete mixtures containing RCAs and dune sand possess, however, inferior mechanical and durability characteristics relative to those of concrete made with natural aggregates (NA) [7–23]. Properties of such a sustainable concrete could be improved through the inclusion of non-metallic fibers into the mixture [24–30]. Such non-metallic fibers, including glass fibers (GF), nylon fibers (NF), polypropylene (PPF), and basalt fibers (BFs), could be used in concrete mixtures in a single-size configuration or in a hybrid combination of different fiber sizes [24–31]. Hybrid non-metallic fibers with different lengths have the potential to restrict the growth of micro- and macro-cracks and improve the properties of concrete mixtures [31]. This study aims to investigate the potential use of hybrid BF to enhance different properties of concrete made with RCAs and dune sand. The hybrid BF combination used consisted of a

blend of 20 and 50 mm long BFs at a ratio of 1:1. In addition to being light, non-magnetic, and non-conductive, BFs are cheaper than glass and carbon fibers [32–37]. The study was supplemented by the numerical modeling of specimens tested in flexure and an inverse analysis of flexural test data, which rendered the development of a new tensile softening law for hybrid BF-reinforced recycled aggregate concrete.

2. Background

Table 1 presents a list of available studies on the behavior of concrete made with RCA. The RCA replacement percentages in these studies were in the range of 20–100%. The cube compressive strength (f_{cu}) of the base concrete adopted in 67% of these studies was 28–43 MPa, while the remaining 26% of the studies included a base cube concrete strength of 49–54 MPa. One study adopted a base cube compressive strength of 102 MPa. The results of previous studies demonstrating the influence of RCA replacement on the properties of plain concrete are plotted in Figure 1. The *y*-axis in Figure 1a–d represents the respective normalized slump (S/S_o), compressive strength ($f_{cu}/f_{cu,o}$), splitting tensile strength ($f_{sp}/f_{sp,o}$), and flexural strength ($f_r/f_{r,o}$) of plain RCA–based mixtures relative to that of a benchmark mixture made with NA. Generally, a slump reduction was recorded with an increase in the RCA replacement percentage, independent of the source of the RCA (Figure 1a). In terms of the compressive strength, Figure 1b shows that for RCA from recycling plants, a gradual reduction in compressive strength was recorded with an increasing RCA replacement percentage. An RCA replacement of more than 25 and 50% was detrimental to the compressive strength of concrete made with RCAs and obtained from CDW and laboratory concrete waste, respectively. Figure 1c shows that there was a gradual reduction in the splitting tensile strength with an increase in the RCA replacement percentage for concrete made with RCAs from recycling plants and laboratory waste. The data obtained by Andreu and Miren [38] from the CDW category showed, however, no splitting tensile strength reductions for the RCA–based concrete mixtures, possibly because of the high strength of the parent concrete from which the RCAs were obtained (crushed high-strength concrete from a pre-cast factory). Figure 1d shows a reduction in the flexural strength with an increase in the RCA replacement percentage, irrespective of the source of the RCAs used.

Table 1. Studies on the effect of RCAs on concrete properties.

Reference	Source of RCA	RCA Replacement (%)	Base Concrete Strength (f_{cu}) (MPa)
Yang et al. [7]	Recycling plant	100	54
Togay et al. [8]	Recycling plant	25, 50, 100	41
Kou and Poon [9]	Recycling facility	20, 50, 100	49
Çakır [10]	Waste processing corporation	25, 50, 75, 100	42
Kachouh et al. [11,12]	Recycling plant	30, 70, 100	43
Malešev et al. [13]	Lab concrete waste	50, 100	43
Katz [14]	Concrete cubes	100	42
Tabsh and Abdelfatah [15]	Lab concrete waste	100	36
Abd Elhakam et al. [16]	Lab concrete waste	25, 50, 75, 100	28
Shaikh and Nguyen [17] [1]	Local CDW	25, 50	51
Rao et al. [18]	Demolished RCC culvert	25, 50, 100	49
Xiao et al. [19]	Airport runway waste	30, 50, 70, 100	36
Saravanakumar et al. [20]	Old-demolished structure	100	36
Zhang et al. [21]	Building material company	100	38
Andreu and Miren [38]	Pre-cast factory specimens	20, 50, 100	102

[1] Cylinder strength was converted to cube strength assuming $f'_c = 0.80 f_{cu}$ [39].

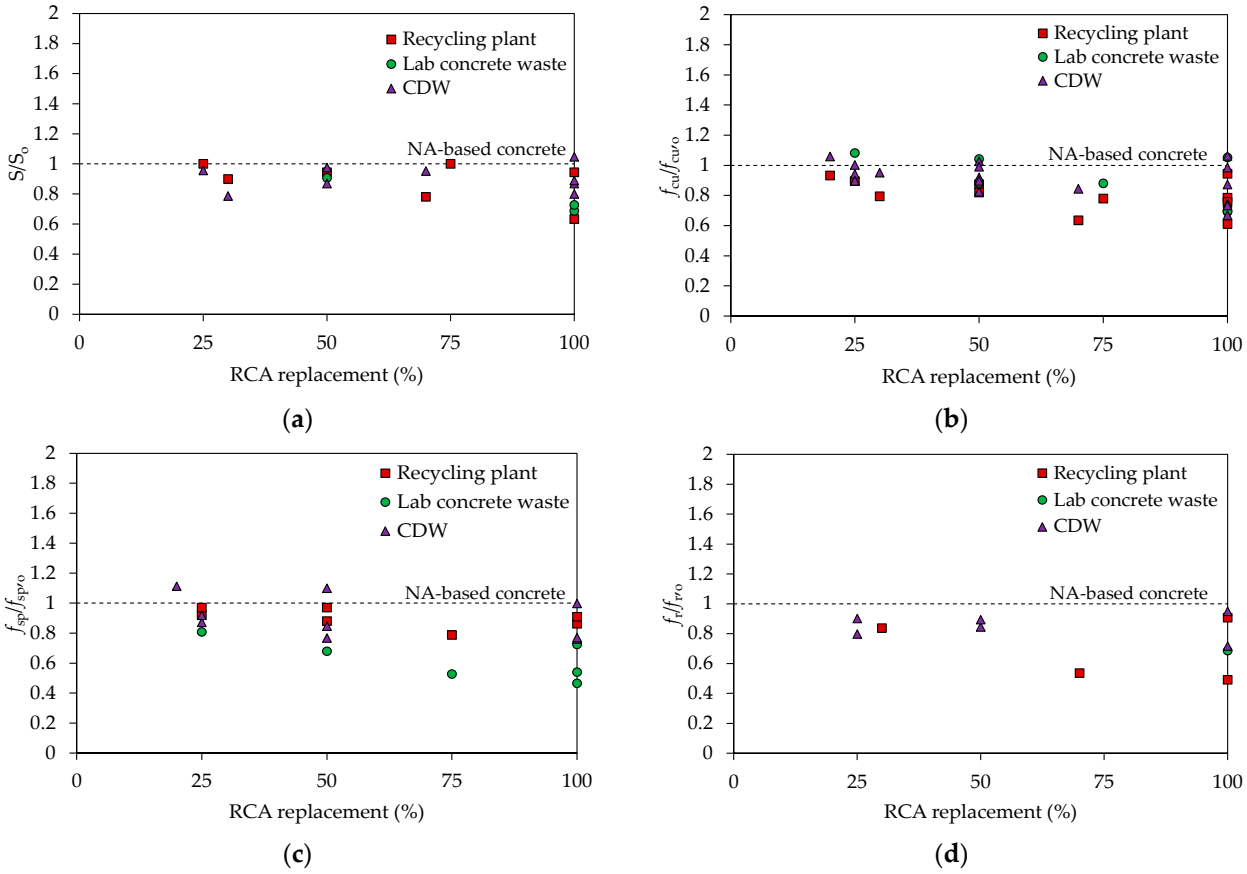


Figure 1. Effect of RCA on concrete properties: (**a**) slump; (**b**) compressive strength; (**c**) splitting tensile strength; (**d**) flexural strength.

Figure 2 shows the impact of varying the base concrete strength on the properties of concrete made with RCA. The slump reduction for the RCA–based mixtures with different base concrete strengths was insignificantly different (Figure 2a). In contrast, the strength reduction caused by an up to 50% RCA replacement percentage tended to be higher for the mixtures with a base concrete strength of 49–54 MPa than for those with a base strength of 28–43 MPa (Figure 2b,c). The mixtures with a base concrete strength of 102 MPa exhibited no strength reduction due to the use of RCA from crushed high-strength concrete [38]. At 100% RCA, mixtures with a lower base concrete strength of 28–43 MPa tended to exhibit greater strength reductions than those of the mixtures with a higher base concrete strength of 49–54 MPa. Such a variation in the trend could be attributed to the source of RCA and the inadequacy of the available data to draw meaningful conclusions.

Non-metallic fibers have the potential to offset the probable degradation in the properties of concrete caused by RCA. Table 2 lists the data of available studies carried out to examine the mechanical properties of RCA–based concrete reinforced with non-metallic fibers. Figure 3 demonstrates the influence of non-metallic fibers on the properties of RCA–based concrete tested in previous studies. The *y*-axis in Figure 3a–d represents the respective normalized slump (S_f/S_o), compressive strength ($f_{cu,f}/f_{cu,o}$), splitting tensile strength ($f_{sp,f}/f_{sp,o}$), and flexural strength ($f_{r,f}/f_{r,o}$) of RCA–based mixtures reinforced with non-metallic fibers relative to that of the benchmark plain mixture made with NA. It is evident from Figure 3a that the addition of non-metallic fibers had a negative impact on the concrete workability, irrespective of the RCA replacement percentage. The RCA replacement percentage did not have a noticeable impact on the slump reduction caused by the fibers. Contrarily, the detrimental effect of the addition of fibers on the slump tended to be more pronounced with an increase in the fiber volume fraction. Figure 3b shows that the compressive strength of the fiber-reinforced concrete mixtures with an RCA

replacement percentage ≤ 25% was almost the same as that of the NA-based plain mixture. Increasing the value of ν_f did not increase the ratio of $f_{cu,f}/f_{cu,o}$. For the mixtures with 25% < RCA ≤ 50%, the addition of non-metallic fibers up to a ν_f of 0.75% was effective in restoring the original compressive strength of NA-based concrete. A further increase in the fiber volume fraction resulted in a decay in the compressive strength. In fact, the ratio of $f_{cu,f}/f_{cu,o}$ for these mixtures with ν_f > 0.75% was consistently less than unity. The concrete mixtures with 50% < RCA ≤ 100% exhibited a trend similar to that of the mixtures with 25% < RCA ≤ 50. Figure 3c shows that the inclusion of non-metallic fibers at ν_f > 0.25% was effective in restoring the original splitting tensile strength of the NA-based mixture for the groups with RCA ≤ 25% and 25% < RCA ≤ 50%. For mixtures of these two groups, the ratio of $f_{sp,f}/f_{sp,o}$ tended to increase with an increase in ν_f. The mixtures with 50% < RCA ≤ 100% exhibited a different trend, where 45% of the data reported that the addition of non-metallic fibers helped in restoring the original splitting tensile strength of the NA-based mixture, while 55% of data demonstrated the ineffectiveness of the fibers in restoring the original splitting tensile strength of the NA-based mixture. Figure 3d shows that the value of $f_{r,f}/f_{r,o}$ was ≥1 for all mixtures with RCA ≤ 25%, indicating an effective restoration of the original flexural strength. The value of $f_{r,f}/f_{r,o}$ further increased with an increase in ν_f. Although the original flexural strength of the NA-based mixture for the specimens with 25% < RCA ≤ 50% was fully restored due to the addition of fibers, increasing ν_f had no effect on the flexural strength gain, where $f_{r,f}/f_{r,o}$ remained constantly close to unity. The effectiveness of non-metallic fibers in restoring the original flexural strength of the NA-based mixture for the specimens with 50% < RCA ≤ 100% was uncertain; this is because 40% of the test data for the mixtures of this group had a $f_{r,f}/f_{r,o} \geq 1$, confirming the full restoration of the original strength, while the remaining 60% had a $f_{r,f}/f_{r,o} < 1$, indicating no or the partial restoration of the original strength.

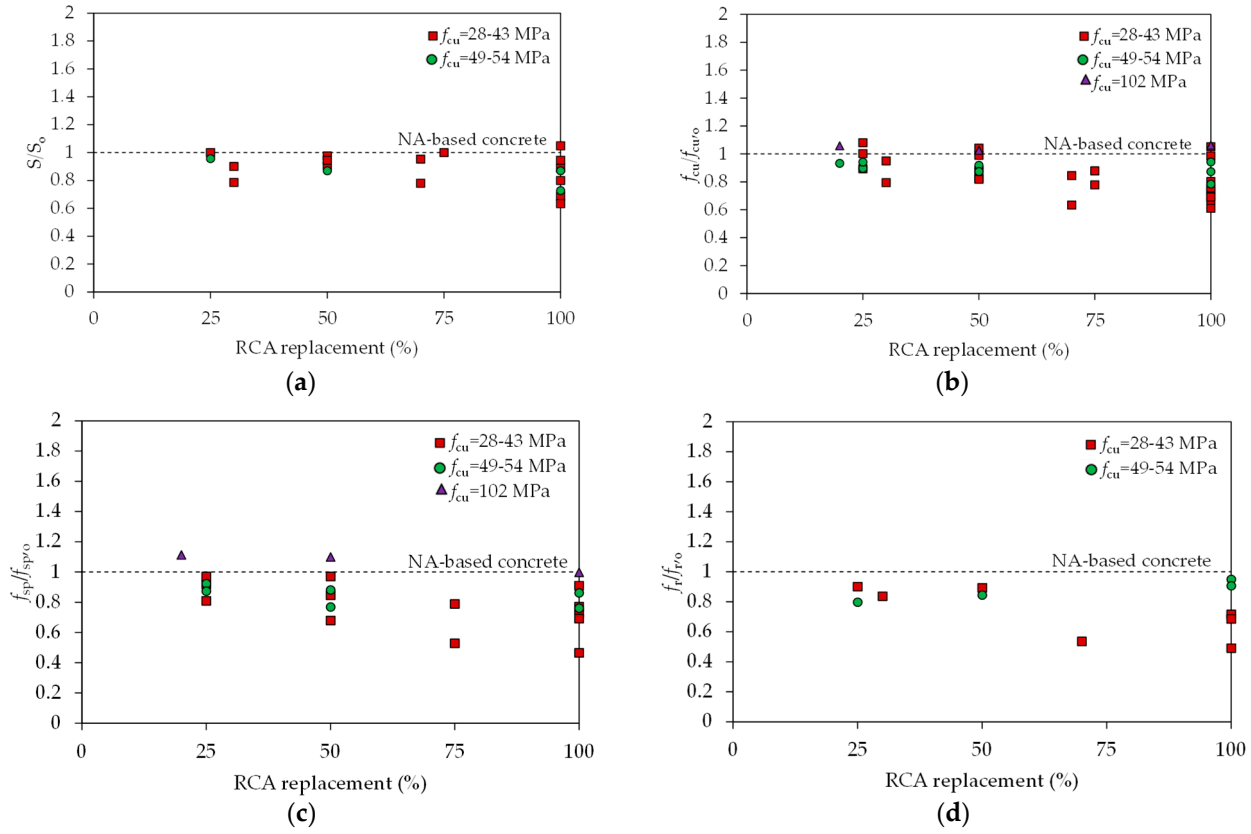


Figure 2. Effect of base concrete compressive strength on properties of RCA–based concrete: (**a**) slump; (**b**) compressive strength; (**c**) splitting tensile strength; (**d**) flexural strength.

Table 2. Studies on the effect of non-metallic fibers on the properties of RCA–based concrete.

Reference	Source of RCA	RCA Replacement (%)	Base Concrete Strength (f_{cu}) (MPa)	Properties of Fibers			
				Type	E_f [1] (GPa)	L_f/d_f [2]	ν_f (%)
Ali et al. [24]	Lab concrete specimens	100	39	GF	72.0	-	0.25, 0.5, 0.75
Lee [25] [3]	Waste concrete	100	45	NF	5.3	826	0.06, 0.12
Ahmed et al. [26]	Demolished buildings	50, 100	66	PPF	3.3	-	0.15, 0.3, 0.45, 0.6, 0.75, 0.9
Das et al. [27]	Demolished buildings	100	37	PPF	4.0	369	0.5, 0.75, 1
Fang et al. [28] [3]	Abandoned concrete	50	38	BF	88.9	1200	0.05, 0.1, 0.2
Katkhuda and Shatarat [29]	Old concrete beams, slabs	20	23	BF	89.0	1125	0.1, 0.3, 0.5, 1, 1.5
Shoaib et al. [30]	Recycling plant	30, 60	40, 59	BF	44	60	0.5, 1.0, 1.5

[1] E_f = Young's modulus of the fibers. [2] L_f = length of the fibers and d_f = diameter of the fibers. [3] Cylinder strength was converted to cube strength assuming $f'_c = 0.80 f_{cu}$ [39].

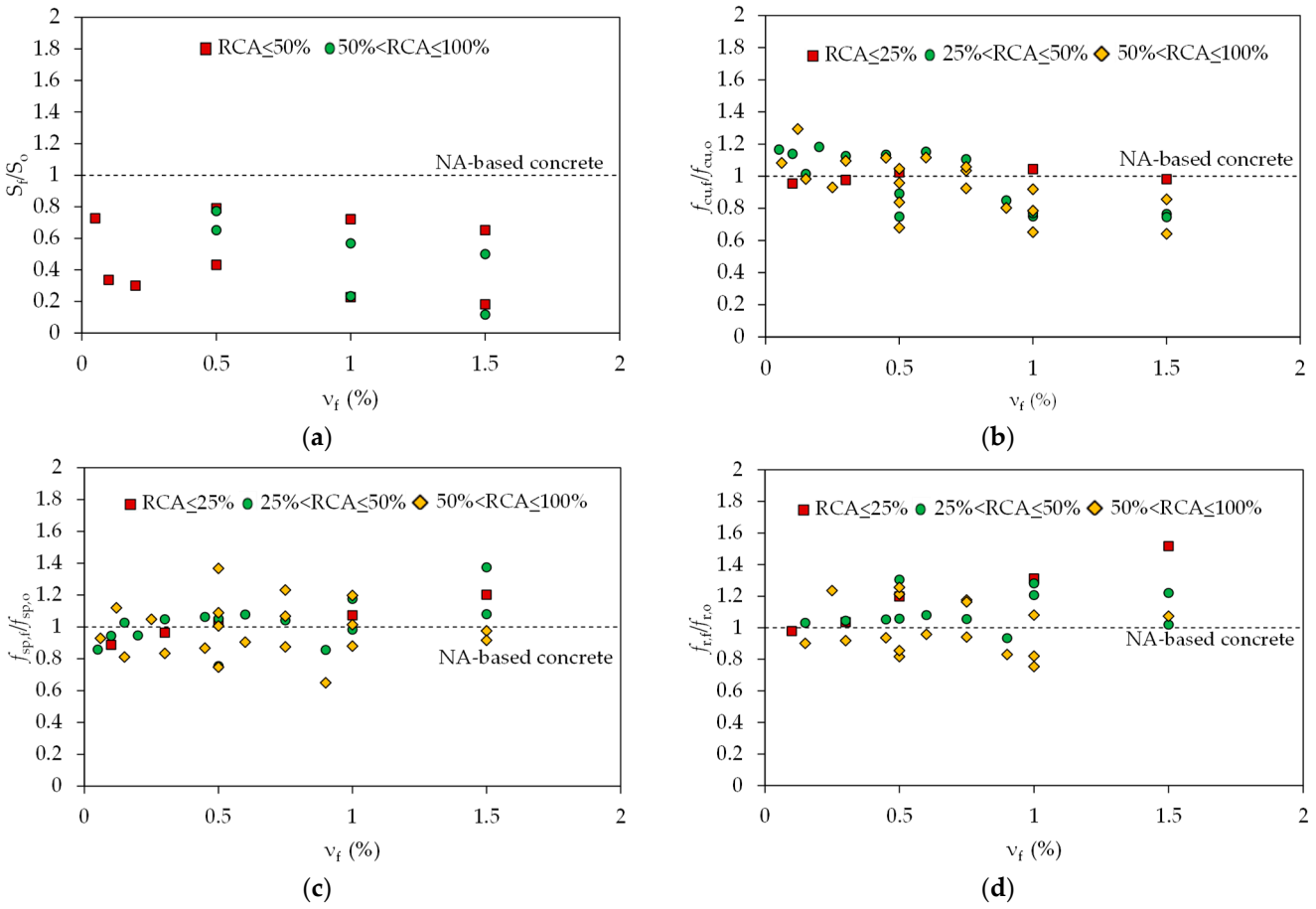


Figure 3. Effect of non-metallic fibers on properties of RCA–based concrete: (**a**) slump; (**b**) compressive strength; (**c**) splitting tensile strength; (**d**) flexural strength.

3. Research Significance

Although previous studies have provided interesting findings on the behavior of RCA–based mixtures reinforced with non-metallic fibers, the interaction between the base concrete grade, RCA replacement percentage, and fiber volume fraction when hybrid non-metallic fibers with different lengths are incorporated into the mixture has not been investigated. A tensile softening law that can describe the post-cracking behavior of hybrid BF-reinforced recycled aggregate concrete is not available. This research aims to fill these research gaps through testing, modeling, and analysis. The new characterization test data and the novel tensile softening law of recycled aggregate concrete reinforced with hybrid BFs offered in the current study will contribute to the widespread use of such a sustainable concrete material, leading to positive impacts on the community and society.

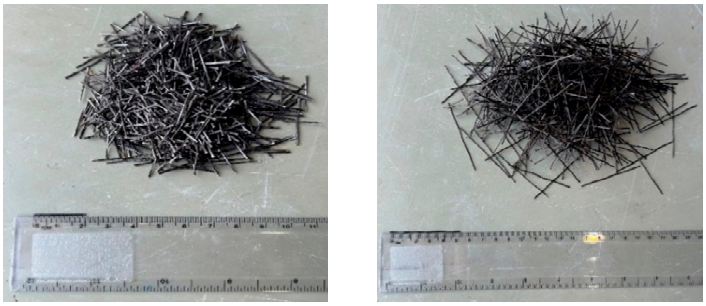
4. Materials

The recycled coarse aggregates were obtained from Al Dhafra Recycling Plant located in Abu Dhabi, UAE, which uses broken concrete from demolished buildings with an undetermined concrete strength to generate well-graded RCAs with a nominal maximum size (NMS) of 25 mm and a particle size distribution conforming to ASTM C33 [40]. The NA were acquired in the form of crushed dolomitic limestone from Stevin Rock, Ras Al Khaimah, UAE, with a NMS of 19 mm. ASTM Type-I Ordinary Portland Cement (OPC) [41] obtained from Emirates Cement Factory, Al Ain, UAE, was used as a binding material. Desert dune sand (DS), obtained from Al Ain Municipality, Al Ain, UAE, was used as the sustainable fine aggregate. The appearance of the coarse and fine aggregates is shown in Figure 4. The workability of the benchmark NSC and HSC mixtures without RCA was maintained in the range of 200–220 mm by adding a superplasticizer (SP) acquired from BASF, Abu Dhabi, UAE. Basalt fibers (BFs) of 20 and 50 mm in length were acquired from ReforceTech AS, Røyken, Norway. The diameter, tensile strength, and elastic modulus of the BFs were 0.72 mm, 900 MPa, and 44 GPa, respectively [42]. Photos of the BFs used are shown in Figure 5. The physical parameters of the aggregates used are listed in Table 3.



(**a**) (**b**) (**c**)

Figure 4. Appearance of aggregates: (**a**) DS; (**b**) NA; (**c**) RCA.



(**a**) (**b**)

Figure 5. Photos of BFs: (**a**) 20 in mm length; (**b**) 50 in mm length.

Table 3. Physical properties of aggregates.

Property	Unit	ASTM Standard	NA	RCA	DS
Absorption	%	C127 [43]	0.40	6.58	-
Specific gravity	-	C127 [43]	2.82	2.63	2.77
Fineness modulus	-	C136 [44]	6.82	7.44	1.45
Surface area	cm^2/g	C136 [44]	2.49	2.50	116.8
Soundness ($MgSO_4$)	%	C88 [45]	1.2	2.78	-
Los Angeles abrasion	%	C131 [46]	16.0	32.6	-
Dry-rodded density	kg/m^3	C29 [47]	1635.0	1563.0	1663.0

5. Methods

5.1. Experimental Program

The test matrix is provided in Table 4. Fifteen concrete mixtures were prepared and divided into two groups based on the base concrete grade (normal-strength concrete (NSC) with a f_{cu} = 40 MPa and high-strength concrete (HSC) with f_{cu} = 60 MPa, noting that concrete with a f_{cu} of 60–100 MPa is defined as a high-strength concrete [48]. The concrete mixtures were labeled as x-Rz-y-b, where x indicates the concrete grade (N for NSC and H for HSC), R means RCA, z stands for RCA replacement percentage (0, 30, 60, and 100), y indicates the presence or absence of fibers (NF for no fibers and HB for hybrid BFs), and b refers to the volume fraction of the hybrid BFs (0.0, 1.0%, and 1.5%).

Table 4. Test matrix.

Grade	Mixture ID [1]	RCA Replacement (%)	BF Volume Fraction (%)
NSC	N-R0-NF-0.0	-	-
	N-R30-NF-0.0	30	-
	N-R60-NF-0.0	60	-
	N-R100-NF-0.0	100	-
	N-R30-HB-1.0	30	1.0
	N-R60-HB-1.0	60	1.0
	N-R60-HB-1.5	60	1.5
	N-R100-HB-1.0	100	1.0
	N-R100-HB-1.5	100	1.5
HSC	H-R0-NF-0.0	-	-
	H-R30-NF-0.0	30	-
	H-R60-NF-0.0	60	-
	H-R30-HB-1.0	30	1.0
	H-R60-HB-1.0	60	1.0
	H-R60-HB-1.5	60	1.5

[1] The hybrid BF combination consisted of a blend of 20 and 50 mm long BFs at a ratio of 1:1.

5.2. Mixture Proportioning and Testing Methods

Table 5 provides the proportions of the concrete mixtures. The preparation of the concrete mixtures began by inserting the RCAs into the concrete mixer in a condition known as saturated surface dry (SSD). Subsequently, the fine aggregates, cement, and natural aggregates, where applicable, were added and mixed for three minutes. Next, water containing SP was added, followed by the addition of the BFs, then this was mixed for an additional three minutes with other constituents. The molds were filled with concrete in five layers. After pouring each concrete layer, the molds were vibrated for five seconds using a horizontal electrical vibrating table. The specimens were wrapped with thick polyethylene sheets to prevent water evaporation, and specimens were demolded after 24 h. The concrete specimens underwent water-curing for 28 days. Table 6 provides details of the specimens and tests adopted in the current study, noting that at least three replicate samples were tested for mechanical properties. It is noteworthy that the length

of the specimens adopted in the current study was three times the larger fiber length, in accordance with ACI 544.2 [49]. The slump test was used to evaluate the workability of the mixtures. The mechanical properties of the mixtures were examined through compression, splitting tensile, and flexural tests. The bulk resistivity and ultrasonic pulse velocity (UPV) tests were used to assess the durability characteristics of the concrete.

Table 5. Mixture proportioning.

Group	Mixture ID	Mass (kg/m^3)							ν_f (%)
		Cement	Sand	NA	RCA	Water	SP	BF	
NSC	N-R0-NF-0.0	470	659	1080	0	230	0.47	0.0	0.0
	N-R30-NF-0.0	470	659	756	324	230	0.47	0.0	0.0
	N-R60-NF-0.0	470	659	432	648	230	0.47	0.0	0.0
	N-R100-NF-0.0	470	659	0	1080	230	0.47	0.0	0.0
	N-R30-HB-1.0	470	659	756	324	230	0.47	21.0	1.0
	N-R60-HB-1.0	470	659	432	648	230	0.47	21.0	1.0
	N-R60-HB-1.5	470	659	432	648	230	0.47	31.5	1.5
	N-R100-HB-1.0	470	659	0	1080	230	0.47	21.0	1.0
	N-R100-HB-1.5	470	659	0	1080	230	0.47	31.5	1.5
HSC	H-R0-NF-0.0	617	513	1080	0	216	0.92	0.0	0.0
	H-R30-NF-0.0	617	513	756	324	216	0.92	0.0	0.0
	H-R60-NF-0.0	617	513	432	648	216	0.92	0.0	0.0
	H-R30-HB-1.0	617	513	756	324	216	0.92	21.0	1.0
	H-R60-HB-1.0	617	513	432	648	216	0.92	21.0	1.0
	H-R60-HB-1.5	617	513	432	648	216	0.92	31.5	1.5

Table 6. Testing procedures and specimen details.

Category	Property	Test Standard	Specimen Details
Fresh	Slump	ASTM C143 [50]	Fresh concrete
Mechanical	Cube compressive strength	BS EN 12390-3:2019 [51]	Cube (150 × 150 mm)
	Cylinder compressive strength	ASTM C39 [52]	Cylinder (150 × 300 mm)
	Elastic modulus	ASTM C469 [53]	Cylinder (100 × 200 mm)
	Splitting tensile strength	ASTM C496 [54]	Cylinder (150 × 300 mm)
	Flexural strength	ASTM C1609 [55]	Prism (100 × 100 × 500 mm)
Durability	Bulk resistivity	ASTM C1760 [56]	Cylinder (100 × 200 mm)
	UPV	ASTM C597 [57]	Cube (150 × 150 mm)

6. Results and Discussion

6.1. Slump

Results of the slump test are shown in Figure 6. The slump of NSC remained unaltered at RCA replacement percentages of 30, 60, and 100%. The slump of HSC mixtures tended to reduce due to the RCA replacement. The addition of hybrid BFs decreased the slump of NSC and HSC. At ν_f of 1.0%, the slump value of NSC made with 30, 60, and 100% decreased by 10, 13, and 7%, respectively. Reductions of 18 and 17% were recorded in the slump value of NSC made with 60 and 100% RCA, respectively, at a hybrid BF ν_f of 1.5%. The slump value of HSC made with 30 and 60% RCA decreased by 14 and 7% at a ν_f of 1.0%, respectively. A slump reduction of 24% was recorded when hybrid BFs were added at ν_f = 1.5% to the HSC mixture made with 60% RCA. The minor slump reduction recorded for the plain specimens with RCA is consistent with other published studies [13,18], where a 4–31% reduction in the concrete slump was recorded due to RCA replacement percentage in the range of 25–100%. The reduction in the slump is attributable to the irregular shape

of RCAs [58,59]. A significant reduction in the slump was recorded in the current study due to the addition of hybrid BFs, and the detrimental effect was more pronounced at ν_f = 1.5%. Such a slump reduction is consistent with other findings in the published data (see Figure 3a), where the addition of non-metallic fibers at ν_f = 0.05–1.5% decreased the slump value of RCA–based concrete by 21–88%.

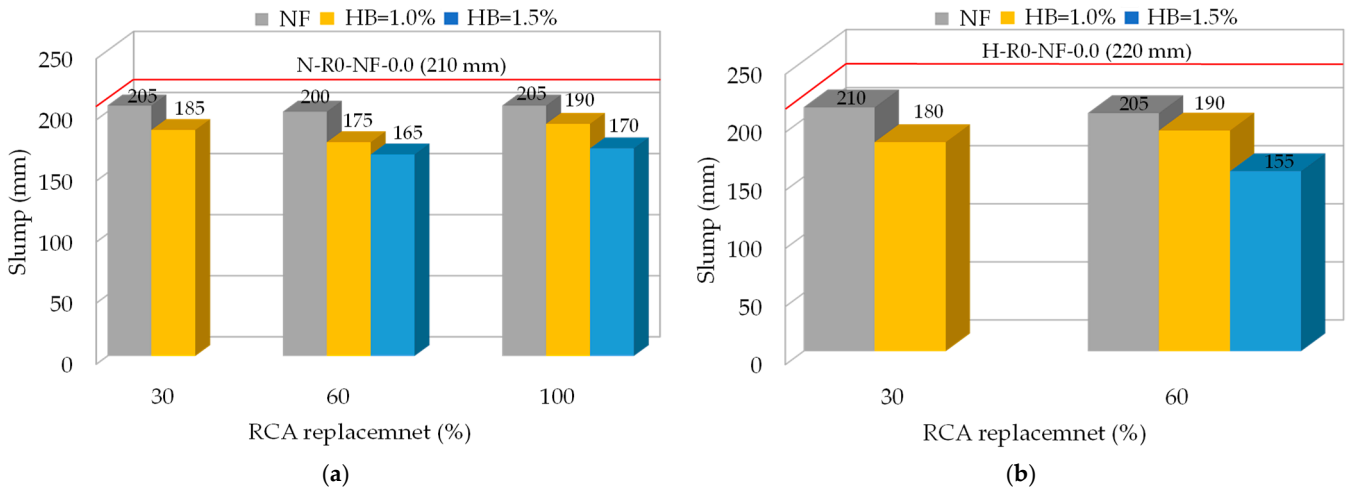


Figure 6. Slump of concrete mixtures: (**a**) NSC; (**b**) HSC.

6.2. Mechanical Properties

Table 7 provides the values of the compressive strength (f_{cu} and f'_c), Young's modulus (E_c), the splitting tensile strength (f_{sp}), and the flexural strength (f_r) of the tested specimens. Photos of the tested specimen samples are provided in Figures 7–9. A discussions of the mechanical test results is provided hereafter.

Table 7. Compression test results of concrete mixtures.

Group	Mixture ID	f_{cu} (MPa) [1]	f'_c (MPa) [1]	E_c (GPa) [1]	f'_c/f_{cu}	f_{sp} (MPa) [1]	f_r (MPa) [1]
NSC	N-R0-NF-0.0	44.9 (2.83)	32.2 (4.33)	30.5 (1.70)	0.72	2.38 (0.27)	3.82 (0.08)
	N-R30-NF-0.0	39.5 (1.10)	27.7 (3.67)	27.6 (1.06)	0.70	2.28 (0.12)	3.90 (0.04)
	N-R60-NF-0.0	35.9 (0.78)	26.5 (3.57)	23.3 (0.02)	0.74	2.00 (0.04)	2.98 (0.32)
	N-R100-NF-0.0	31.2 (0.56)	24.2 (3.78)	17.4 (0.48)	0.78	1.82 (0.05)	2.77 (0.33)
	N-R30-HB-1.0	35.4 (1.70)	25.2 (2.08)	25.4 (4.03)	0.71	2.67 (0.23)	4.01 (0.38)
	N-R60-HB-1.0	28.8 (2.05)	21.1 (2.04)	21.6 (2.62)	0.73	2.27 (0.17)	3.05 (0.36)
	N-R60-HB-1.5	30.2 (1.41)	23.1 (1.11)	28.8 (3.23)	0.77	2.42 (0.15)	3.30 (0.37)
	N-R100-HB-1.0	20.3 (2.11)	16.6 (0.93)	15.5 (0.89)	0.82	1.94 (0.12)	2.87 (0.54)
	N-R100-HB-1.5	22.6 (1.11)	17.2 (2.25)	20.1 (2.19)	0.76	2.41 (0.16)	3.89 (0.49)
HSC	H-R0-NF-0.0	58.2 (0.89)	46.9 (1.14)	39.9 (2.37)	0.81	3.57 (0.09)	4.50 (0.60)
	H-R30-NF-0.0	55.1 (2.35)	42.3 (2.41)	27.9 (2.49)	0.77	2.81 (0.39)	3.65 (0.56)
	H-R60-NF-0.0	41.6 (1.14)	35.6 (1.42)	22.9 (2.41)	0.85	3.52 (0.10)	3.60 (0.57)
	H-R30-HB-1.0	48.3 (2.84)	42.0 (2.17)	32.1 (1.79)	0.87	2.49 (0.34)	4.14 (0.87)
	H-R60-HB-1.0	43.4 (1.10)	36.1 (3.28)	23.8 (0.76)	0.83	2.67 (0.41)	3.97 (0.14)
	H-R60-HB-1.5	49.6 (0.98)	35.2 (3.45)	23.1 (0.60)	0.71	3.13 (0.30)	4.83 (0.08)

[1] Values between parentheses represent the standard deviation.



Figure 7. Sample concrete cubes after compression tests: (**a**) N-R60-NF-0.0; (**b**) N-R60-HB-1.0; (**c**) H-R30-NF-0.0; (**d**) H-R30-HB-1.0.

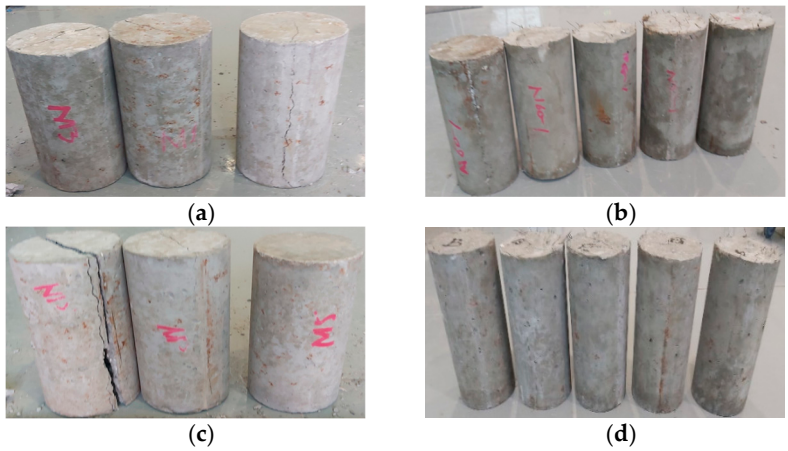


Figure 8. Sample concrete cylinders after splitting tensile test: (**a**) N-R60-NF-0.0; (**b**) N-R60-HB-1.0; (**c**) H-R60-NF-0.0; (**d**) H-R30-HB-1.5.

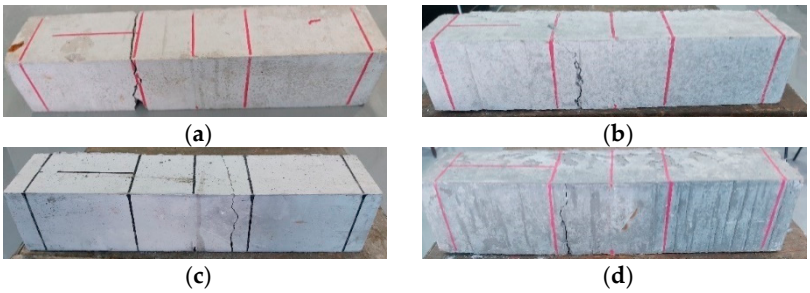


Figure 9. Sample concrete prisms after the flexural test: (**a**) N-R100-NF-0.0; (**b**) N-R100-HB-1.0; (**c**) H-R60-NF-0.0; (**d**) H-R60-HB-1.5.

6.2.1. Compressive Strength

The results of the compressive strength presented in Table 7 indicate that the f_{cu} value of NSC made with 30, 60, and 100% RCA reduced by 12, 20, and 31%, respectively. The HSC specimens exhibited strength reductions of 5 and 29% at RCA replacement percentages of 30 and 60%, respectively. The addition of hybrid BFs did not improve the f_{cu} values of NSC and HSC specimens. In many cases, the addition of hybrid BFs decreased the f_{cu} values of RCA–based concrete mixtures by up to 35 and 12% for NSC and HSC, respectively. The RCA–based HSC mixture made with 60% RCA and hybrid BFs at a ν_f of 1.5% exhibited, however, an increase of 19% in the f_{cu} value relative to that of its RCA–based counterpart. The values of f'_c/f_{cu} listed in Table 7 for all the tested specimens were insignificantly different, implying that the RCAs and hybrid BFs had no noticeable impact on the slenderness effect. The reduction in the compressive strength observed in the

current study due to RCA is consistent with the findings of previous studies [14,16,17,19], where a trend of compressive strength reduction was recorded with an increase in the RCA replacement percentage. The reduction in compressive strength caused by the addition of hybrid BFs in many of the tested specimens is also consistent with other published data [60], where a reduction of up to 19% in f_{cu} was recorded with the addition of hybrid steel–polypropylene fibers. Such a compressive strength reduction could be due to the consumption of some of the available mortar into the wrapping of fibers, the breakage of fibers during the agitation process, and the agglomeration/non-uniform dispersion of fibers into the cementitious matrix, which could have created weak surfaces [28,61]. As such, the use of concrete made with RCAs, with or without BFs, in the concrete columns of high-rise buildings may not be useful, because the use of such a concrete would render columns of a large size, which might not be convenient for owners and users.

6.2.2. Young's Modulus

The results of the Yung's modulus presented in Table 7 show reductions of 10, 24, and 43% in the E_c values of NSC made with 30, 60, and 100% RCA, respectively. The HSC specimens made with 30 and 60% exhibited respective reductions of 30 and 43%. At a hybrid BF value of ν_f = 1.0%, an insignificant effect on the E_c value was recorded for NSC made with 30, 60, and 100% RCA. However, the addition of hybrid BFs at a ν_f = 1.5% improved the E_c of NSC made with 60 and 100% RCA by 24 and 16%, respectively. The E_c value of HSC made with 30% RCA increased by 15% at ν_f = 1.0%. The addition of hybrid BFs had, however, no noticeable effect on the E_c value of HSC made with 60% RCA, irrespective of the fiber volume fraction. The degradation in the E_c values of the NSC and HSC made with RCA replacement is consistent with other published data [62], where a reduction of 11% in the E_c value was recorded at 100% RCA. Additionally, the addition of hybrid BFs tended to improve the E_c values of the NSC and HSC mixtures. This finding is consistent with data reported by Dong et al. [61], where an improvement of 19% in the E_c value of concrete made with 50% RCA was observed due to the addition of a single type of BF.

6.2.3. Splitting Tensile Strength

Figure 10 shows the results of the splitting tensile strength (f_{sp}) of the NSC and HSC specimens tested at 28 days, whereas the corresponding values are listed in Table 7. Figure 10 is important because it provides information on the effectiveness of non-metallic fibers in improving the f_{sp} of RCA–based concrete and the possibility of restoring the original f_{sp} of the NA-based benchmark specimens. The f_{sp} values of the benchmark NSC and HSC specimens are added for comparison purposes. Reductions of 4, 16, and 24% in the f_{sp} values were recorded for NSC made with 30, 60, and 100% RCA, respectively. The HSC specimens made with 30 and 60% RCA exhibited reductions of 21 and 30% in the f_{sp} values, respectively. The addition of hybrid BFs improved the f_{sp} values of the NSC and HSC mixtures. At a hybrid BF ν_f = 1.0%, the f_{sp} values of the NSC made with 30, 60, and 100% RCA improved by 17, 15, and 7%, respectively. At a hybrid BF of ν_f = 1.5%, the f_{sp} values of the NSC made 60 and 100% RCA increased by 20 and 32%, respectively. The HSC specimens made with 30 and 60% RCA exhibited an improvement of 25 and 7% in the f_{sp} value at ν_f = 1.0%. The f_{sp} value of HSC made with 60% RCA improved by 26% at ν_f = 1.5%.

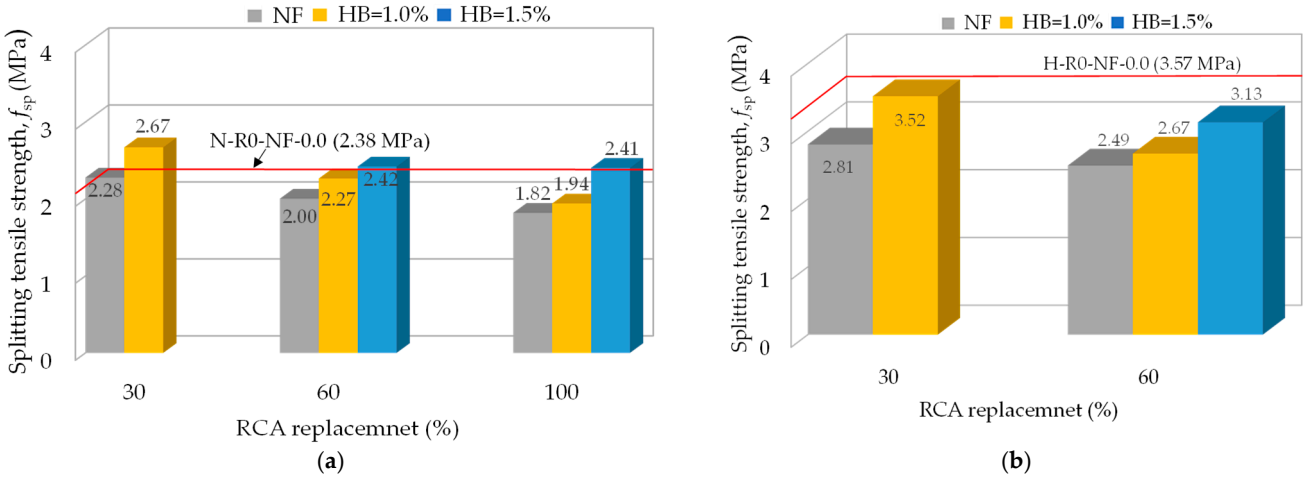


Figure 10. Splitting tensile strength test results: (**a**) NSC; (**b**) HSC.

The degradation in the f_{sp} of the plain HSC specimens due to RCA was more significant than that of their NSC counterparts. The addition of hybrid BFs was more impactful to the f_{sp} of the NSC than HSC. At 30% RCA, the use of hybrid BFs at ν_f = 1.0% fully restored the f_{sp} of the original NA-based benchmark NSC mixture. At 60 and 100% RCA, it was necessary to add hybrid BFs at ν_f = 1.5% to fully restore the original f_{sp} of the NA-based benchmark NSC mixture. The use of hybrid BFs at ν_f = 1.0% in HSC made with 30 and 60% RCA restored 99 and 75% of the original f_{sp} of the NA-based benchmark HSC mixture. The addition of hybrid BFs at ν_f = 1.5% to HSC made with 60% RCA restored 88% of the original f_{sp} of the NA-based benchmark HSC mixture.

In the current study, the reduction in the f_{sp} values with RCA replacement is consistent with other reported results (see Figure 1c), where a reduction in the f_{sp} values was noticed with RCA replacement. The increase in f_{sp} with the addition of hybrid BFs is consistent with other published data [63], where the f_{sp} of concrete made with 100% RCA increased by up to 52% with the addition of hybrid steel–polypropylene fibers. Contrarily, some of the studies [28,61] reported that the addition of a single type of non-metallic fiber had a negative effect on the f_{sp} of RCA–based concrete. Fang et al. [28] observed a reduction of up to 16% in the f_{sp} value of concrete made with 100% RCA due to the addition of BFs at a ν_f of 0.05–0.2%. Dong et al. [61] reported a decrease of up to 33% in the f_{sp} of concrete made with 50% RCA due to the use of BFs at ν_f = 0.1%. Therefore, it might be preferable to use fibers in a hybrid form to improve the splitting tensile strength of RCA–based concrete.

6.2.4. Flexural Properties

The results of the flexural strength (f_r) of the NSC and HSC specimens are shown in Figure 11, whereas the corresponding values are listed in Table 7. Figure 11 is important because it provides information on the effectiveness of non-metallic fibers improving the f_r of RCA–based concrete and the possibility of restoring the original f_r of the NA-based benchmark specimens. The f_r value of NSC made with 30% RCA did not decrease. However, reductions of 22 and 27% were recorded in the f_r values of NSC made with 60 and 100% RCA, respectively. The f_r values of HSC made with 30 and 60% RCA decreased by 19 and 20%, respectively. The use of hybrid BFs improved the f_r values of the NSC and HSC mixtures. At a ν_f of 1.0%, insignificant improvements of 3, 2, and 4% were recorded in the f_r value of NSC made with 30, 60, and 100% RCA, respectively. Furthermore, an increase of 11 and 40% in the f_r value was noticed for NSC made with 60 and 100% RCA at ν_f = 1.5%. The HSC specimens made with 30 and 60% RCA exhibited strength increments of 13 and 10% in the f_r values at ν_f = 1.0%. However, the f_r value of HSC made with 60% RCA increased by 34% at ν_f of 1.5%. It is noteworthy that the plain NSC and HSC specimens failed in a brittle manner at the onset of the initiation of the flexural crack due to the absence of reinforcing fibers, which diminished the tension-stiffening effect. These

specimens failed at zero deflection at peak load with null flexural toughness. Such a brittle mode of failure occurs suddenly without warning, which may lead to catastrophic failure in practical setting. The use of hybrid BFs improved the load capacity and post-peak behavior of the NSC and HSC specimens. The typical load-deflection responses of hybrid BF-reinforced NSC and HSC specimens made with 60% RCA are shown in Figure 12. The flexural toughness (T_{150}^{D}) of hybrid BF-reinforced NSC and HSC mixtures is compared in Figure 13. With a hybrid BF value of ν_f = 1.0%, the flexural toughness values of NSC mixtures made with 30, 60, and 100% RCA were 8.72, 5.83, and 5.97 J, respectively. These results indicate that increasing the RCA replacement percentage from 30 to 60% reduced the flexural toughness of the mixtures made with hybrid BFs (ν_f = 1%) by 33%. A further increase in the RCA replacement percentage did not result in an additional reduction in the flexural toughness. Increasing the hybrid BF volume fraction from 1 to 1.5% improved the flexural toughness of the hybrid BF-reinforced NSC mixtures made with 60 and 100% RCA by 16 and 19%, respectively. The flexural toughness of the HSC mix reinforced with hybrid BFs at ν_f = 1.0% decreased from 6.87 and 6.39 J (7%) due to the increase in the RCA replacement percentage from 30 to 60%. The addition of hybrid BFs at ν_f = 1.5% increased the flexural toughness of the HSC mixture made with 60% RCA by 20%, relative to that of its counterpart with a ν_f of 1.0%.

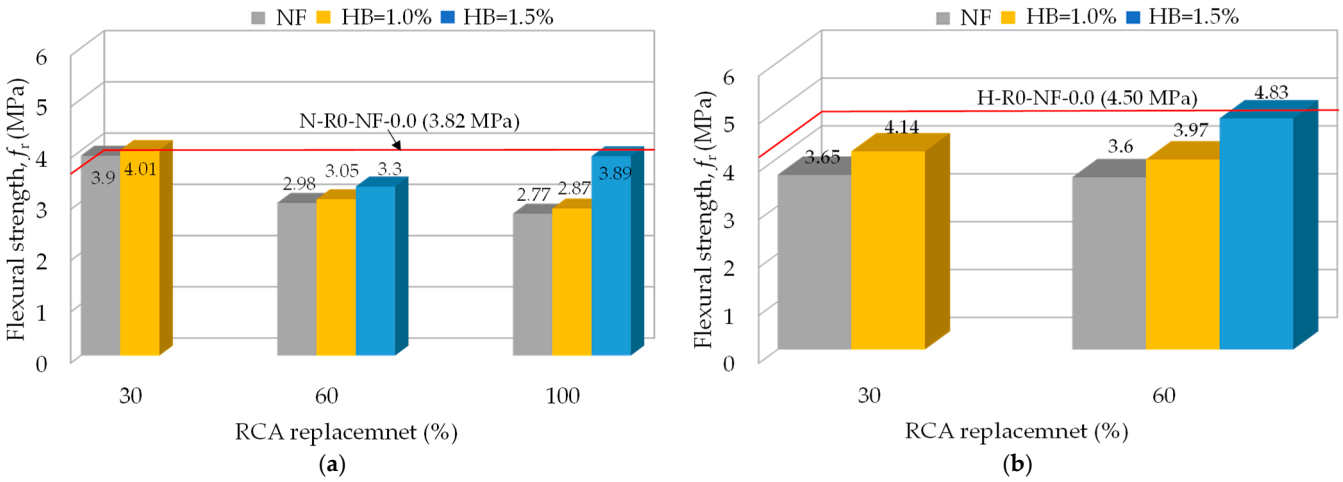


Figure 11. Flexural strength test results: (**a**) NSC; (**b**) HSC.

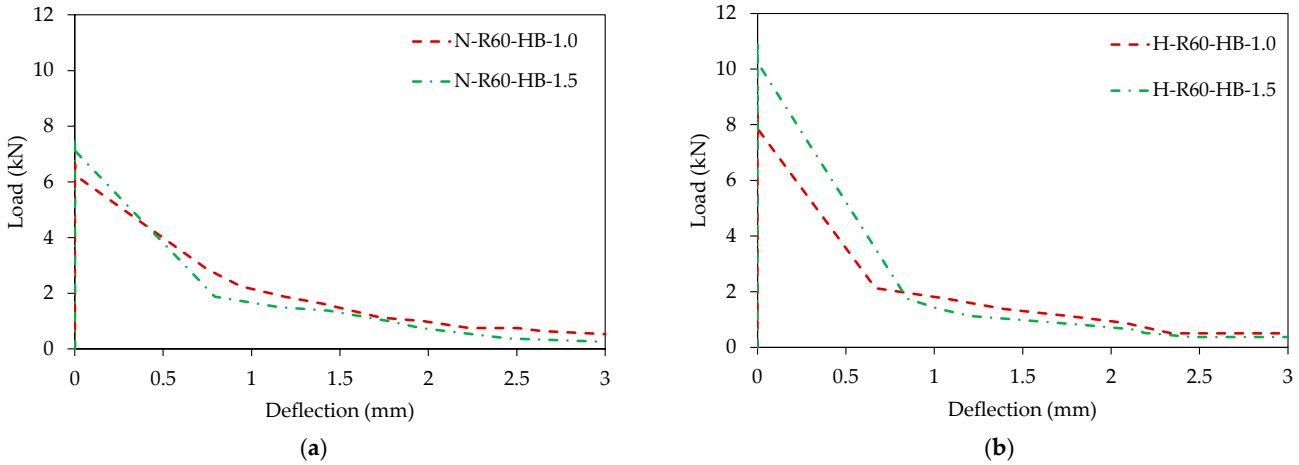


Figure 12. Load-deflection response of hybrid BF-reinforced concrete made with 60% RCA: (**a**) NSC; (**b**) HSC.

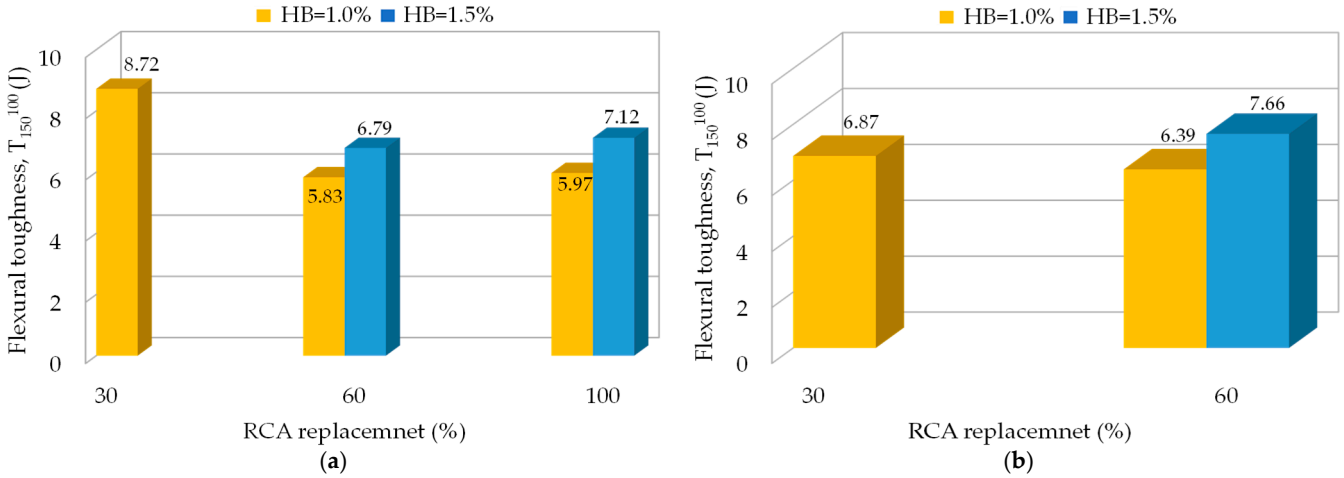


Figure 13. Flexural toughness of hybrid BF-reinforced mixtures: (**a**) NSC; (**b**) HSC.

In the current study, the RCA replacement reduced the flexural strength of NSC and HSC mixtures, except for N-R30-NF-0.0. The rate of degradation in the flexural strength at 60% RCA replacement percentage was insignificantly different for the NSC and HSC mixtures. Such a reduction in the flexural strength due to RCA is consistent with other published data (see Figure 1d), where a reduction in the flexural strength was reported with an increase in the RCA replacement percentage. The use of hybrid BFs improved the flexural strength of the NSC and HSC mixtures in the current study. In a previous study [30], it was reported that the use of a single type of BF with a length of 43 mm resulted in a strength decay in some cases. It is interesting to report that the use of hybrid BFs at ν_f = 1.5% in this study did not result in a flexural strength decay. In fact, it was necessary to use hybrid BFs at ν_f = 1.5% in some cases to fully restore the original flexural strength of the NA-based mixture, noting that a minimum of 86% of the original flexural strength was restored in all other cases. These findings highlight the advantage of using non-metallic BFs in a hybrid form rather than as a single type.

6.3. Durability Properties

6.3.1. Bulk Resistivity

The results of the bulk resistivity of the NSC and HSC specimens are shown in Figure 14. The RCA replacement was detrimental to concrete bulk resistivity. The level of corrosion protection can be estimated based on the bulk resistivity test data [64]. The level of the corrosion protection of the NA-based benchmark specimens N-R0-NF-0.0 and H-R0-NF-0.0 was "Low-to-Moderate". The bulk resistivity of the NSC specimens was reduced by 13, 14, and 16% at RCA replacement percentages of 30, 60, and 100%, respectively, relative to that of N-R0-NF-0.0. Reductions of 19 and 32% were recorded in the bulk resistivity of HSC made with 30 and 60% RCA, respectively, relative to that of the H-R0-NF-0.0. The level of the corrosion protection of the NSC mixture made with 30% RCA was maintained as "Low-to-Moderate", while that of its counterparts made with 60 and 100% RCA replacement became "Low". Despite the reduction in their bulk resistivity, the corrosion protection of the plain RCA–based HSC remained "Low-to-Moderate". The addition of hybrid BFs had no noticeable effect on the bulk resistivity, and hence, the level of corrosion of the hybrid BF-reinforced mixtures remained the same as that of their plain counterparts.

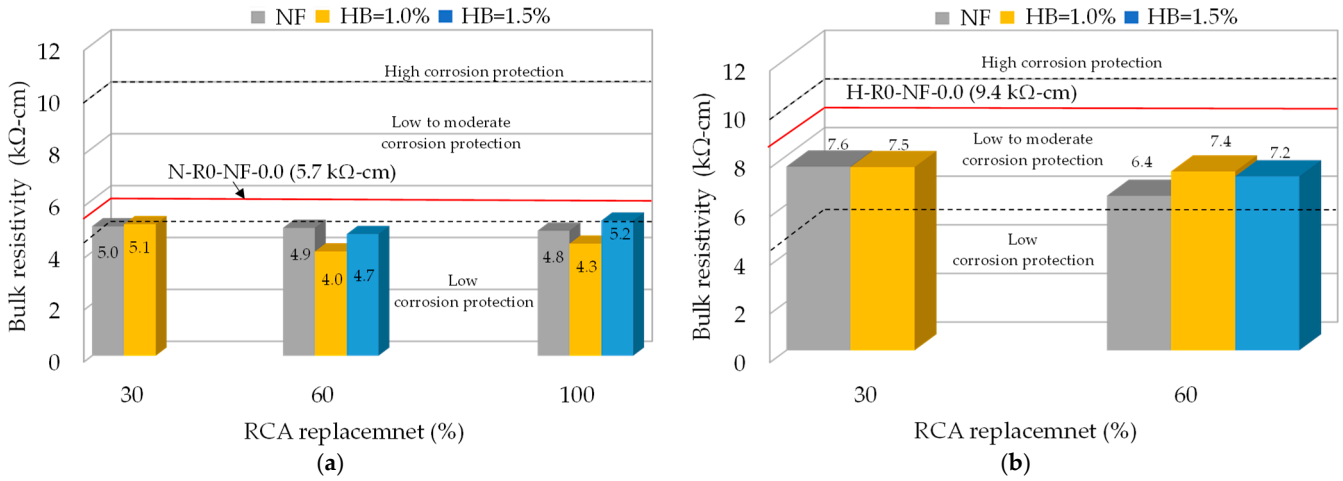


Figure 14. Bulk resistivity results: (**a**) NSC; (**b**) HSC.

6.3.2. Ultrasonic Pulse Velocity

Pulse velocity testing measures the transit time of an ultrasonic pulse through the concrete. The denser the concrete, the higher the velocity (i.e., less transit time) [65]. The test should be, however, conducted with caution in practical setting because the results are affected by the presence of steel reinforcing bars [65]. The results of the UPV test are demonstrated in Figure 15. The quality of the NA-based benchmark specimens N-R0-NF-0.0 and H-R0-NF-0.0 was esteemed as "Excellent". No reduction in the concrete quality was recorded at 30% RCA for both NSC and HSC. Nevertheless, the concrete quality of the mixtures with 60 and 100% RCA was reduced to "Good". The addition of hybrid BFs had no noticeable effect on the UPV of the mixtures. Some hybrid BF-reinforced concrete mixtures exhibited no or a minor increase in their UPV. Other hybrid BF-reinforced concrete mixtures, particularly those of the NSC made with 100% RCA, exhibited a reduction. As such, the rating of the concrete quality of the hybrid BF-reinforced concrete mixtures remained the same as that of their plain counterparts.

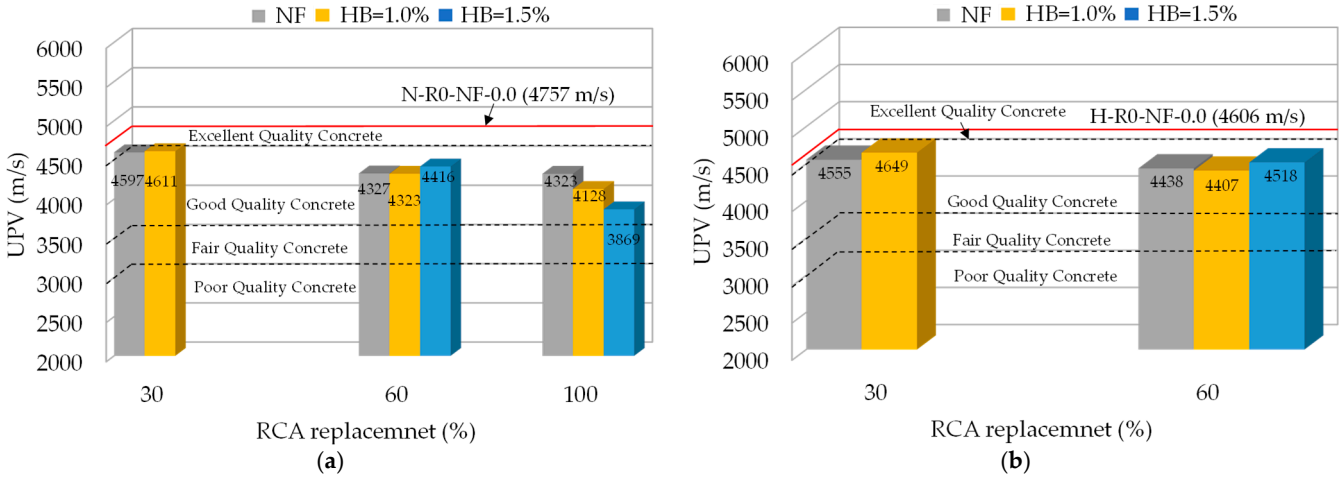


Figure 15. Ultrasonic pulse velocity test results: (**a**) NSC; (**b**) HSC.

7. Development of Tensile Softening Law

The RCA–based mixtures reinforced with hybrid BFs showed improved tensile properties and post-cracking responses relative to those of their plain counterparts. It is essential to develop a tensile softening law (tension function) that is capable of reflecting such an improvement caused by hybrid BFs. This information is critical for the precise analysis and design of structural elements that are made of such a sustainable concrete. The develop-

ment of the tension function demands numerical modeling and an inverse analysis of the flexural test data.

7.1. Simualtion Model

Three-dimensional (3D) simulation models were created using ATENA software [66] for concrete prisms tested under four-point bending. Half of the concrete prism was modeled to minimize the computational time. The manual of the software [66] recommends using a minimum of four to six elements in the shortest dimension of the member to ensure solution convergence within a reasonable time frame. As such, a maximum mesh size of 15 mm was used, which rendered a total of 833 concrete macro-elements elements and 3332 nodes for the half-model. Steel plates at the load and support points were included in the simulation models to avoid a stress concentration. The bottom plate was prevented from movement in transverse and vertical directions using a line support. The movement of the plane of symmetry was restrained in the longitudinal direction using surface supports. A vertical displacement was induced incrementally at the mid-point of the top steel plate. The load at the mid-point of the top plate and the deflection at the midspan were recorded using monitoring points. The software [66] adopts a default multilinear function in compression, which is based on the cylinder compressive strength and Young's modulus of the concrete. The tension function that was used in the analysis is presented in the following section. Figure 16a shows the geometry and boundary conditions of a typical simulation model, whereas Figure 16b shows a typical deformed shape at peak load.

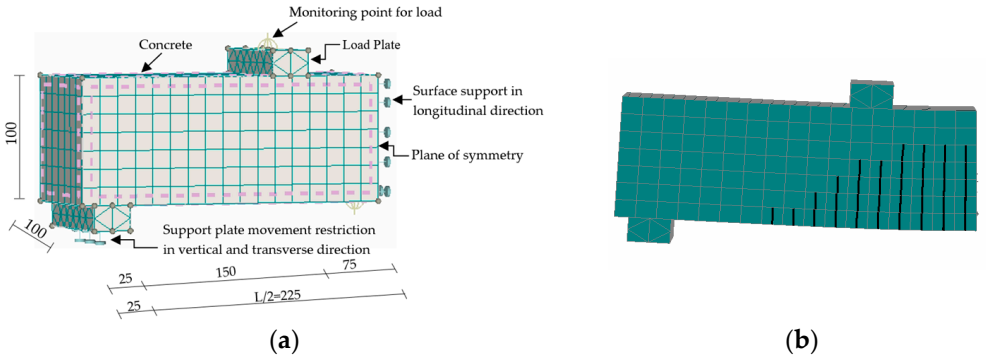


Figure 16. Numerical model: (**a**) geometry and boundary conditions; (**b**) typical deformed shape.

7.2. Tensile Softening Law

Based on an inverse analysis of the flexural test data, the normalized tension function given by Equation (1) and shown schematically in Figure 17a was developed for the concrete mixtures reinforced with hybrid BFs. The symbols f_t, σ_{res}, σ_t, and ε_t denote the uniaxial tensile strength, residual tensile stress, tensile stress, and tensile strain, respectively. The value of f_t was taken as $\frac{4}{9}f_r$ [67]. Numerous iterations were carried out to determine the breaking points of the tension function. Figure 17b,c shows the respective tension functions of BF-reinforced NSC and HSC.

$$\sigma_{res} = \frac{\sigma_t}{f_t} = \begin{cases} 1 - 200\varepsilon_t & \varepsilon_t \leq 0.002 \\ 0.638 - 19.44\varepsilon_t & 0.002 \leq \varepsilon_t \leq 0.02 \\ 0.341 - 4.55\varepsilon_t & 0.02 \leq \varepsilon_t \leq 0.075 \end{cases} \quad (1)$$

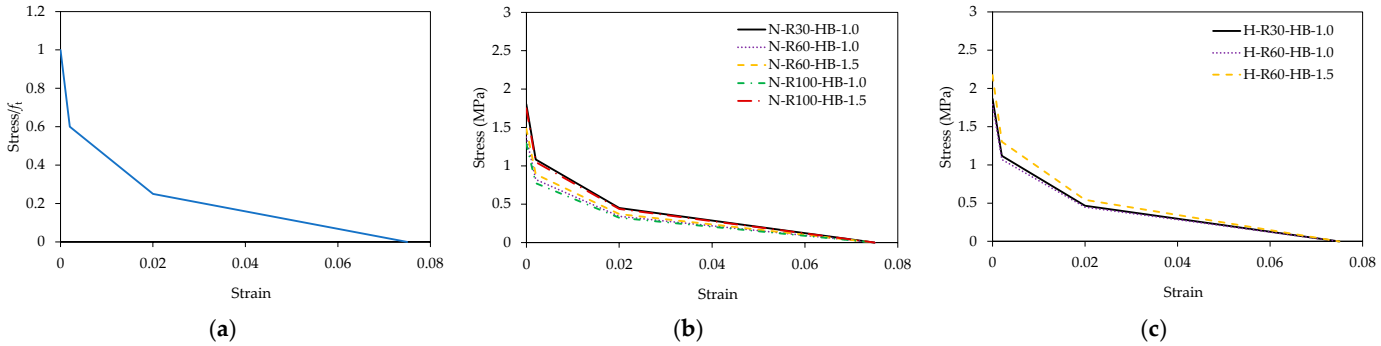


Figure 17. Tensile softening laws: (**a**) Normalized laws; (**b**) NSC; (**c**) HSC.

7.3. Validation of the Tensile Softening Law

The predicted and experimental load-deflection responses of the NSC and HSC demonstrated a consistent pattern, as shown in Figure 18 and Figure 19, respectively. Table 8 presents a comparison of the load capacity, and the flexural toughness predicted numerically, and those obtained from the tests. Such a comparison is important to validate the accuracy of the tensile softening law developed in this study and implemented in the simulation models. The percentage error in predicting the load capacity was less than 10%, whereas that of the flexural toughness was within the 28.3% error band. The good agreement between the predicted and experimental results verifies the accuracy and validity of the tensile softening law established in the present study.

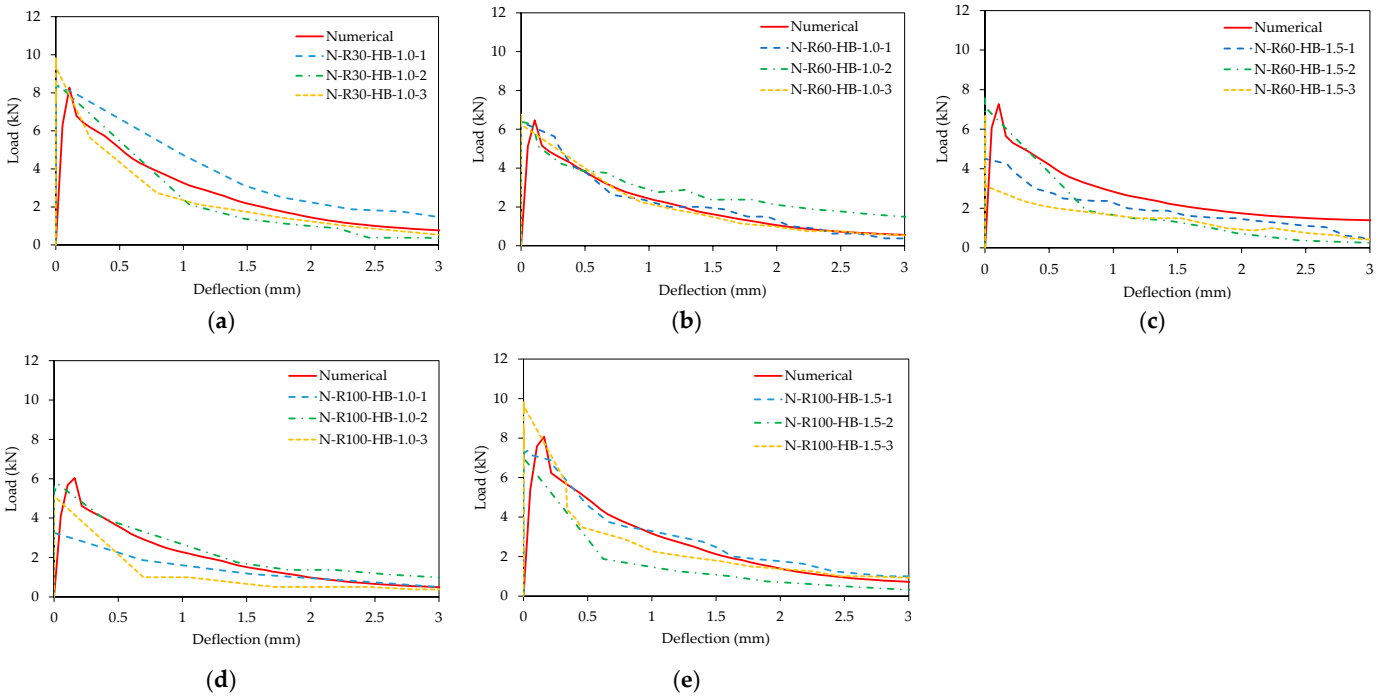


Figure 18. Numerical versus experimental load-deflection responses of NSC: (**a**) N-R30-HB-1.0; (**b**) N-R60-HB-1.0; (**c**) N-R60-HB-1.5; (**d**) N-R100-HB-1.0; (**e**) N-R100-HB-1.5.

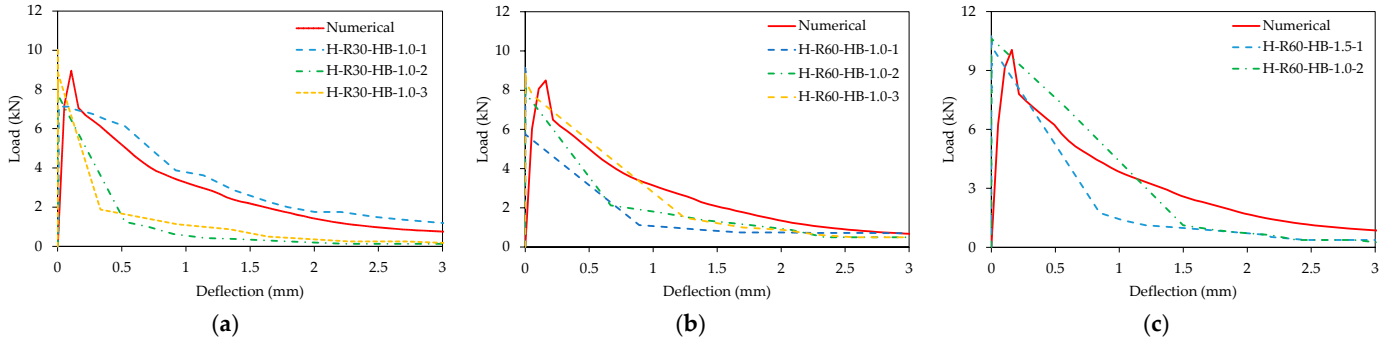


Figure 19. Numerical versus experimental load-deflection responses of HSC: (**a**) H-R30-HB-1.0; (**b**) H-R60-HB-1.0; (**c**) H-R60-HB-1.5.

Table 8. Comparison between experimental and numerical results.

Mixture ID	Load Capacity (KN)		Toughness (J)		Error [1] (%)	
	Experimental	Numerical	Experimental	Numerical	Load Capacity	Toughness
N-R30-HB-1.0	8.91	8.27	8.72	8.30	−7.2	−4.8
N-R60-HB-1.0	6.77	6.47	5.83	6.20	−4.4	6.3
N-R60-HB-1.5	7.33	7.27	6.79	7.96	−0.8	17.2
N-R100-HB-1.0	6.37	6.03	5.97	5.82	−5.3	−2.5
N-R100-HB-1.5	8.65	8.07	7.12	8.02	−6.7	12.6
H-R30-HB-1.0	9.21	8.95	6.87	8.39	−2.8	22.1
H-R60-HB-1.0	8.82	8.50	6.39	8.07	−3.6	26.3
H-R60-HB-1.5	10.74	10.05	7.66	9.83	−6.4	28.3

[1] Error (%) $= \frac{\text{Numerical} - \text{Experimental}}{\text{Experimental}} \times 100$.

8. Conclusions

The properties of the NSC and HSC mixtures made with RCAs with and without hybrid BFs were evaluated. New tensile softening laws for describing the post-cracking response of RCA–based concrete mixtures reinforced with hybrid BFs were developed and verified. The main conclusions of the work are summarized herein:

Effect of RCAs on properties of plain concrete mixtures

- The inclusion of RCAs in plain concrete mixtures insignificantly reduced the slump of the NSC and HSC mixtures.
- Plain NSC mixtures made with 30, 60, and 100% RCA exhibited cube compressive strength reductions of 12, 20, and 31%, respectively. The HSC specimens exhibited cube compressive strength reductions of 5 and 29% at 30 and 60% RCA, respectively.
- Splitting tensile strength reductions of 4, 16, and 24% were recorded for the NSC mixtures at 30, 60, and 100% RCA, respectively. The HSC mixtures exhibited higher splitting tensile strength reductions of 21 and 30% when made with 30 and 60% RCA, respectively.
- Flexural strength reductions of 22 and 27% were recorded for NSC made with 60 and 100% RCA, respectively. The flexural strengths of the HSC mixtures made with 30 and 60% RCA were 19 and 20% lower than that of the NA-based benchmark HSC mixture.
- The bulk resistivity of the plain NSC mixtures decreased by 13, 14, and 16% at RCA of 30, 60, and 100%, respectively. Reductions of 19 and 32% were recorded in the bulk resistivity of HSC at 30 and 60% RCA, respectively.
- Based on UPV test data, no change in the category of the concrete quality "Excellent" was recorded at 30% RCA for both NSC and HSC. At 60 and 100% RCA, the concrete quality category was reduced from "Excellent" to "Good".

Effect of hybrid BFs on properties of RCA–based concrete mixtures

- The inclusion of hybrid BFs reduced the slump by up to 18 and 24% for the NSC and HSC mixtures.
- The use of hybrid BFs did not improve the compressive strength of RCA–based mixtures, except in one case where an increase of 19% was recorded for the HSC mixture with 60% RCA and a ν_f of 1.5%. In many other cases, the addition of hybrid BFs decreased the compressive strength by up to 35 and 12% for NSC and HSC, respectively.
- The use of hybrid BFs at ν_f = 1.0% was sufficient to fully restore the original splitting tensile strength of the NSC with 30 and 60% RCA. At 100% RCA, it was necessary to use hybrid BFs at ν_f = 1.5% to restore the original splitting tensile strength. For HSC made with 30% RCA, the addition of hybrid BFs at ν_f = 1.0% restored the original splitting tensile strength. For HSC made with 60% RCA, only 75 and 88% of the original splitting tensile strength could be restored when hybrid BFs were used at a ν_f of 1.0 and 1.5%, respectively.
- The use of hybrid BFs at ν_f = 1.0% could not fully restore the original flexural strength of the NSC and HSC with 60% RCA. It was necessary to use hybrid BFs at ν_f = 1.5% in NSC made with 100% RCA and HSC made with 60% RCA in order to fully restore the original flexural strength of the corresponding NA-based mixture.
- Increasing the ν_f of the hybrid BFs from 1 to 1.5% improved the flexural toughness of the NSC with 60 and 100% RCA by 16 and 19%, respectively. The use of hybrid BFs at ν_f = 1.5% increased the flexural toughness of HSC made with 60% RCA by 20%, relative to that of its counterpart with ν_f of 1.0%.
- The addition of hybrid BFs had no noticeable effect on the bulk resistivity. As a result, the level of corrosion of the hybrid BF-reinforced mixtures remained the same as that of their plain counterparts. Similarly, the use of hybrid BFs had no noticeable effect on the UPV, and hence, the rating of the concrete quality of the hybrid BF-reinforced concrete mixtures remained the same as that of their plain counterparts.

Development of new tensile softening law

- New idealized tensile softening laws were established for hybrid BF-reinforced recycled aggregate concrete. The tensile softening laws were implemented into numerical models to simulate the flexural behavior of the tested concrete prisms. The flexural responses predicted numerically were in good agreement with the experimental results.

Author Contributions: Conceptualization, T.E.-M., H.E.-H. and S.S.; methodology, T.E.-M., H.E.-H. and S.S.; software, S.S. and T.E.-M., validation, S.S. and T.E.-M.; formal analysis, S.S., T.E.-M. and H.E.-H.; investigation, S.S., T.E.-M. and H.E.-H.; resources, T.E.-M. and H.E.-H.; data curation, S.S.; writing—original draft preparation, S.S.; writing—review and editing, T.E.-M., H.E.-H. and S.S.; visualization, S.S.; supervision, T.E.-M. and H.E.-H.; project administration, T.E.-M.; funding acquisition, T.E.-M. All authors have read and agreed to the published version of the manuscript.

Funding: This project is funded by the United Arab Emirates University (UAEU) [grant number 12N004].

Data Availability Statement: The data presented in this study are available on request from the corresponding author. The data are not publicly available due to privacy issues.

Conflicts of Interest: The authors declare no conflict of interest.

References

1. Radonjanin, V.; Malešev, M.; Marinković, S.; Al Malty, A.E.S. Green Recycled Aggregate Concrete. *Constr. Build. Mater.* **2013**, *47*, 1503–1511. [CrossRef]
2. Kabirifar, K.; Mojtahedi, M.; Wang, C.; Tam, V.W.Y. Construction and Demolition Waste Management Contributing Factors Coupled with Reduce, Reuse, and Recycle Strategies for Effective Waste Management: A Review. *J. Clean. Prod.* **2020**, *263*, 121265. [CrossRef]
3. Bandow, N.; Gartiser, S.; Ilvonen, O.; Schoknecht, U. Evaluation of the Impact of Construction Products on the Environment by Leaching of Possibly Hazardous Substances. *Environ. Sci. Eur.* **2018**, *30*, 14. [CrossRef] [PubMed]
4. Bakaeva, N.V.; Klimenko, M.Y. Technique for Reduction of Environmental Pollution from Construction Wastes. *IOP Conf. Ser. Mater. Sci. Eng.* **2017**, *262*, 012195. [CrossRef]

5. Masood, A.; Ahmad, T.; Arif, M.; Mahdi, F. Waste Management Strategies for Concrete. *Environ. Eng. Policy* **2001**, *3*, 15–18. [CrossRef]
6. Safiuddin, M.; Alengaram, U.J.; Rahman, M.M.; Salam, M.A.; Jumaat, M.Z. Use of Recycled Concrete Aggregate in Concrete: A Review. *J. Civ. Eng. Manag.* **2013**, *19*, 796–810. [CrossRef]
7. Yang, J.; Du, Q.; Bao, Y. Concrete with Recycled Concrete Aggregate and Crushed Clay Bricks. *Constr. Build. Mater.* **2011**, *25*, 1935–1945. [CrossRef]
8. Ozbakkaloglu, T.; Gholampour, A.; Xie, T. Mechanical and Durability Properties of Recycled Aggregate Concrete: Effect of Recycled Aggregate Properties and Content. *J. Mater. Civ. Eng.* **2018**, *30*, 04017275. [CrossRef]
9. Kou, S.C.; Poon, C.S. Enhancing the Durability Properties of Concrete Prepared with Coarse Recycled Aggregate. *Constr. Build. Mater.* **2012**, *35*, 69–76. [CrossRef]
10. Çakır, Ö. Experimental Analysis of Properties of Recycled Coarse Aggregate (RCA) Concrete with Mineral Additives. *Constr. Build. Mater.* **2014**, *68*, 17–25. [CrossRef]
11. Kachouh, N.; El-Hassan, H.; El-Maaddawy, T. Effect of Steel Fibers on the Performance of Concrete Made with Recycled Concrete Aggregates and Dune Sand. *Constr. Build. Mater.* **2019**, *213*, 348–359. [CrossRef]
12. Kachouh, N.; El-Hassan, H.; El-Maaddawy, T. Influence of Steel Fibers on the Flexural Performance of Concrete Incorporating Recycled Concrete Aggregates and Dune Sand. *J. Sustain. Cem.-Based Mater.* **2021**, *10*, 165–192. [CrossRef]
13. Malešev, M.; Radonjanin, V.; Marinković, S. Recycled Concrete as Aggregate for Structural Concrete Production. *Sustainability* **2010**, *2*, 1204–1225. [CrossRef]
14. Katz, A. Properties of Concrete Made with Recycled Aggregate from Partially Hydrated Old Concrete. *Cem. Concr. Res.* **2003**, *33*, 703–711. [CrossRef]
15. Tabsh, S.W.; Abdelfatah, A.S. Influence of Recycled Concrete Aggregates on Strength Properties of Concrete. *Constr. Build. Mater.* **2009**, *23*, 1163–1167. [CrossRef]
16. Abd Elhakam, A.; Mohamed, A.E.; Awad, E. Influence of Self-Healing, Mixing Method and Adding Silica Fume on Mechanical Properties of Recycled Aggregates Concrete. *Constr. Build. Mater.* **2012**, *35*, 421–427. [CrossRef]
17. Shaikh, F.U.A.; Nguyen, H.L. Properties of Concrete Containing Recycled Construction and Demolition Wastes as Coarse Aggregates. *J. Sustain. Cem.-Based Mater.* **2013**, *2*, 204–217. [CrossRef]
18. Chakradhara Rao, M.; Bhattacharyya, S.K.; Barai, S.V. Influence of Field Recycled Coarse Aggregate on Properties of Concrete. *Mater. Struct.* **2011**, *44*, 205–220. [CrossRef]
19. Xiao, J.; Li, J.; Zhang, C. Mechanical Properties of Recycled Aggregate Concrete under Uniaxial Loading. *Cem. Concr. Res.* **2005**, *35*, 1187–1194. [CrossRef]
20. Saravanakumar, P.; Abhiram, K.; Manoj, B. Properties of Treated Recycled Aggregates and Its Influence on Concrete Strength Characteristics. *Constr. Build. Mater.* **2016**, *111*, 611–617. [CrossRef]
21. Zhang, H.; Ji, T.; Liu, H.; Su, S. Modifying Recycled Aggregate Concrete by Aggregate Surface Treatment Using Sulphoaluminate Cement and Basalt Powder. *Constr. Build. Mater.* **2018**, *192*, 526–537. [CrossRef]
22. Al-Harthy, A.S.; Halim, M.A.; Taha, R.; Al-Jabri, K.S. The Properties of Concrete Made with Fine Dune Sand. *Constr. Build. Mater.* **2007**, *21*, 1803–1808. [CrossRef]
23. Dawood, A.O.; Jaber, A.M. Effect of Dune Sand as Sand Replacement on the Mechanical Properties of the Hybrid Fiber Reinforced Concrete. *Civ. Environ. Eng.* **2022**, *18*, 111–136. [CrossRef]
24. Ali, B.; Qureshi, L.A.; Raza, A.; Nawaz, M.A.; Rehman, S.U.; Rashid, M.U. Influence of Glass Fibers on Mechanical Properties of Concrete with Recycled Coarse Aggregates. *Civ. Eng. J.* **2019**, *5*, 1007–1019. [CrossRef]
25. Lee, S. Effect of Nylon Fiber Addition on the Performance of Recycled Aggregate Concrete. *Appl. Sci.* **2019**, *9*, 767. [CrossRef]
26. Ahmed, T.W.; Ali, A.A.M.; Zidan, R.S. Properties of High Strength Polypropylene Fiber Concrete Containing Recycled Aggregate. *Constr. Build. Mater.* **2020**, *241*, 118010. [CrossRef]
27. Das, C.S.; Dey, T.; Dandapat, R.; Mukharjee, B.B.; Kumar, J. Performance Evaluation of Polypropylene Fibre Reinforced Recycled Aggregate Concrete. *Constr. Build. Mater.* **2018**, *189*, 649–659. [CrossRef]
28. Fang, S.-E.; Hong, H.-S.; Zhang, P.-H. Mechanical Property Tests and Strength Formulas of Basalt Fiber Reinforced Recycled Aggregate Concrete. *Materials* **2018**, *11*, 1851. [CrossRef]
29. Katkhuda, H.; Shatarat, N. Shear Behavior of Reinforced Concrete Beams Using Treated Recycled Concrete Aggregate. *Constr. Build. Mater.* **2016**, *125*, 63–71. [CrossRef]
30. Shoaib, S.; El-Maaddawy, T.; El-Hassan, H.; El-Ariss, B.; Alsalami, M. Characteristics of Basalt Macro-Fiber Reinforced Recycled Aggregate Concrete. *Sustainability* **2022**, *14*, 14267. [CrossRef]
31. Zuaiter, M.; El-Hassan, H.; El-Maaddawy, T.; El-Ariss, B. Properties of Slag-Fly Ash Blended Geopolymer Concrete Reinforced with Hybrid Glass Fibers. *Buildings* **2022**, *12*, 1114. [CrossRef]
32. Sim, J.; Park, C.; Moon, D.Y. Characteristics of Basalt Fiber as a Strengthening Material for Concrete Structures. *Compos. Part B Eng.* **2005**, *36*, 504–512. [CrossRef]
33. Li, Z.; Ma, J.; Ma, H.; Xu, X. Properties and Applications of Basalt Fiber and Its Composites. *IOP Conf. Ser. Earth Environ. Sci.* **2018**, *186*, 012052. [CrossRef]
34. Dhand, V.; Mittal, G.; Rhee, K.Y.; Park, S.-J.; Hui, D. A Short Review on Basalt Fiber Reinforced Polymer Composites. *Compos. Part B Eng.* **2015**, *73*, 166–180. [CrossRef]

35. Larrinaga, P.; Chastre, C.; Biscaia, H.C.; San-José, J.T. Experimental and Numerical Modeling of Basalt Textile Reinforced Mortar Behavior under Uniaxial Tensile Stress. *Mater. Des.* **2014**, *55*, 66–74. [CrossRef]
36. Li, Y.; Zhang, J.; He, Y.; Huang, G.; Li, J.; Niu, Z.; Gao, B. A Review on Durability of Basalt Fiber Reinforced Concrete. *Compos. Sci. Technol.* **2022**, *225*, 109519. [CrossRef]
37. Ahmed, W.; Lim, C.W. Production of Sustainable and Structural Fiber Reinforced Recycled Aggregate Concrete with Improved Fracture Properties: A Review. *J. Clean. Prod.* **2021**, *279*, 123832. [CrossRef]
38. Andreu, G.; Miren, E. Experimental Analysis of Properties of High Performance Recycled Aggregate Concrete. *Constr. Build. Mater.* **2014**, *52*, 227–235. [CrossRef]
39. *BS EN 206-1:2000*; Concrete—Part 1: Specification, performance, production and conformity. British Standards: London, UK, 2000.
40. Standard Specification for Concrete Aggregates. Available online: https://www.astm.org/c0033_c0033m-18.html (accessed on 27 March 2023).
41. *ASTM C150/C150M—19a*; Standard Specification for Portland Cement. ASTM International: West Conshohocken, PA, USA, 2012.
42. ReforceTech AS, Røyken, Norway. Available online: https://reforcetech.com/ (accessed on 15 January 2023).
43. *ASTM C127-15*; Standard Test Method for Relative Density (Specific Gravity) and Absorption of Coarse Aggregate. ASTM International: West Conshohocken, PA, USA, 2015.
44. *ASTM C136/C136M-19*; Test Method for Sieve Analysis of Fine and Coarse Aggregates. ASTM International: West Conshohocken, PA, USA, 2020.
45. *ASTM C88/C88M-18*; Standard Test Method for Soundness of Aggregates by Use of Sodium Sulfate or Magnesium Sulfate. ASTM International: West Conshohocken, PA, USA, 2018.
46. *ASTM C131-06*; Standard Test Method for Resistance to Degradation of Small-Size Coarse Aggregate by Abrasion and Impact in the Los Angeles Machine. ASTM International: West Conshohocken, PA, USA, 2006.
47. *ASTM C29/C29M-17a*; Test Method for Bulk Density (Unit Weight) and Voids in Aggregate. ASTM International: West Conshohocken, PA, USA, 2017.
48. Concrete Society. *TR 49 Design Guidance for High Strength Concrete*; Concrete Society: Berkshire, UK, 1998.
49. American Concrete Institute. *ACI 544.2R-17: Report on the Measurement of Fresh State Properties and Fiber Dispersion of Fiber-Reinforced Concrete*; American Concrete Institute: Farmington Hills, MI, USA, 2017.
50. *ASTM C 143*; Test Method for Slump of Hydraulic-Cement Concrete. ASTM International: West Conshohocken, PA, USA, 2012.
51. *BS EN 12390-3:2019*; Testing Hardened Concrete. Compressive Strength of Test Specimens. British Standards: London, UK, 2019.
52. *ASTM C39*; Test Method for Compressive Strength of Cylindrical Concrete Specimens. ASTM International: West Conshohocken, PA, USA, 2018.
53. *ASTM C469-02*; Test Method for Static Modulus of Elasticity and Poissons Ratio of Concrete in Compression. ASTM International: West Conshohocken, PA, USA,, 2014.
54. *ASTM C496/C496M-17*; Test Method for Splitting Tensile Strength of Cylindrical Concrete Specimens. ASTM International: West Conshohocken, PA, USA, 2017.
55. *ASTM C1609/C1609M-19a*; Test Method for Flexural Performance of Fiber-Reinforced Concrete (Using Beam with Third-Point Loading). ASTM International: West Conshohocken, PA, USA, 2010.
56. *ASTM 1760-19*; Standard Test Method for Bulk Electrical Resistivity or Bulk Conductivity of Concrete. ASTM International: West Conshohocken, PA, USA.
57. *ASTM C597*; Standard Test Method for Pulse Velocity Through Concrete. ASTM International: West Conshohocken, PA, USA, 2016.
58. Wagih, A.M.; El-Karmoty, H.Z.; Ebid, M.; Okba, S.H. Recycled Construction and Demolition Concrete Waste as Aggregate for Structural Concrete. *HBRC J.* **2013**, *9*, 193–200. [CrossRef]
59. Ismail, S.; Ramli, M. Engineering Properties of Treated Recycled Concrete Aggregate (RCA) for Structural Applications. *Constr. Build. Mater.* **2013**, *44*, 464–476. [CrossRef]
60. Tahmouresi, B.; Koushkbaghi, M.; Monazami, M.; Abbasi, M.T.; Nemati, P. Experimental and Statistical Analysis of Hybrid-Fiber-Reinforced Recycled Aggregate Concrete. *Comput. Concr.* **2019**, *24*, 193–206. [CrossRef]
61. Dong, J.F.; Wang, Q.Y.; Guan, Z.W. Material Properties of Basalt Fibre Reinforced Concrete Made with Recycled Earthquake Waste. *Constr. Build. Mater.* **2017**, *130*, 241–251. [CrossRef]
62. Etxeberria, M.; Vázquez, E.; Marí, A.; Barra, M. Influence of Amount of Recycled Coarse Aggregates and Production Process on Properties of Recycled Aggregate Concrete. *Cem. Concr. Res.* **2007**, *37*, 735–742. [CrossRef]
63. He, W.; Kong, X.; Fu, Y.; Zhou, C.; Zheng, Z. Experimental Investigation on the Mechanical Properties and Microstructure of Hybrid Fiber Reinforced Recycled Aggregate Concrete. *Constr. Build. Mater.* **2020**, *261*, 120488. [CrossRef]
64. ACI 222R 01. Protection of Metals in Concrete Against Corrosion. In *ACI Manual for Concrete Practice*; American Concrete Institute: Farmington Hills, MI, USA, 2008.
65. Ratay, R.T. *Structural Condition Assessment*; Wiley: Hoboken, NJ, USA, 2005.

66. ATENA Computer Software. Cervenka Consulting s.r.o.: Prague, Czech Republic. Available online: https://www.cervenka.cz/products/atena/ (accessed on 18 January 2023).
67. Ashour, S.A.; Hasanain, G.S.; Wafa, F.F. Shear Behavior of High-Strength Fiber Reinforced Concrete Beams. *Struct. J.* **1992**, *89*, 176–184. [CrossRef]

Disclaimer/Publisher's Note: The statements, opinions and data contained in all publications are solely those of the individual author(s) and contributor(s) and not of MDPI and/or the editor(s). MDPI and/or the editor(s) disclaim responsibility for any injury to people or property resulting from any ideas, methods, instructions or products referred to in the content.